Society For Biomaterials

In vitro evaluation of decellularized ECM-derived surgical scaffold biomaterials

Xiao Luo,[1,2†] Katherine M. Kulig,[1†] Eric B. Finkelstein,[1,3] Margaret F. Nicholson,[1] Xiang-Hong Liu,[4] Scott M. Goldman,[4] Joseph P. Vacanti,[5,6] Brian E. Grottkau,[6,7] Irina Pomerantseva,[1,5,6] Cathryn A. Sundback,[1,5,6‡] Craig M. Neville[1,5,6,7‡]

[1]Center for Regenerative Medicine, Massachusetts General Hospital, Boston, Massachusetts 02114
[2]Tongji Hospital, Huazhong University of Science and Technology, Wuhan, Hubei 434300, People's Republic of China
[3]The Department of Biomedical and Chemical Engineering, Syracuse Biomaterials Institute, Syracuse University, Syracuse, New York 13244
[4]DSM Biomedical, Exton, Pennysylvania 19341
[5]Department of Surgery, Massachusetts General Hospital, Boston, Massachusetts 02114
[6]Harvard Medical School, Boston, Massachusetts 02115
[7]Department of Orthopaedic Surgery, Massachusetts General Hospital, Boston, Massachusetts 02114

Received 24 June 2015; revised 19 October 2015; accepted 2 November 2015
Published online 00 Month 2015 in Wiley Online Library (wileyonlinelibrary.com). DOI: 10.1002/jbm.b.33572

Abstract: Decellularized extracellular matrix (ECM) biomaterials are increasingly used in regenerative medicine for abdominal tissue repair. Emerging ECM biomaterials with greater compliance target surgical procedures like breast and craniofacial reconstruction to enhance aesthetic outcome. Clinical studies report improved outcomes with newly designed ECM scaffolds, but their comparative biological characteristics have received less attention. In this study, we investigated scaffolds derived from dermis (AlloDerm Regenerative Tissue Matrix), small intestinal submucosa (Surgisis 4-layer Tissue Graft and OASIS Wound Matrix), and mesothelium (Meso BioMatrix Surgical Mesh and Veritas Collagen Matrix) and evaluated biological properties that modulate cellular responses and recruitment. An assay panel was utilized to assess the ECM scaffold effects upon cells. Results of the material-conditioned media study demonstrated Meso BioMatrix and OASIS best supported cell proliferation. Meso BioMatrix promoted the greatest migration and chemotaxis signaling, followed by Veritas and OASIS; OASIS had superior suppression of cell apoptosis. The direct adhesion assay indicated that AlloDerm, Meso BioMatrix, Surgisis, and Veritas had sidedness that affected cell-material interactions. In the chick chorioallantoic membrane assay, Meso BioMatrix and OASIS best supported cell infiltration. Among tested materials, Meso BioMatrix and OASIS demonstrated characteristics that facilitate scaffold incorporation, making them promising choices for many clinical applications. © 2015 Wiley Periodicals, Inc. J Biomed Mater Res Part B: Appl Biomater 00B: 000–000, 2015.

Key Words: extracellular matrix, scaffolds, cell adhesion, cell proliferation, in vitro

How to cite this article: Luo X, Kulig KM, Finkelstein EB, Nicholson MF, Liu X-H, Goldman SM, Vacanti JP, Grottkau BE, Pomerantseva I, Sundback CA, Neville CM. 2015. *In vitro* evaluation of decellularized ECM-derived surgical scaffold biomaterials. J Biomed Mater Res Part B 2015:00B:000–000.

INTRODUCTION

The extracellular matrix (ECM) is derived from secreted proteins, and includes highly structured and cross-linked fibers, glycosaminoglycans, latent signaling molecules, and proteases with processing and remodeling roles. Biological surgical scaffolds generated from residual ECM following tissue decellularization are increasingly being used to facilitate soft tissue repair in many clinical settings.[1–5] The ECM materials are derived from a variety of tissues (small intestine, dermis, mesothelium, peritoneum, heart valve, bladder, and brain[6–12]) and species (bovine, porcine, equine, and human). Considerable variation exists between tissues and even species, which impacts resulting properties. Consequently, although the biological scaffolds may appear similar, significant differences arise in various clinical settings.

Although the primary role of the surgical scaffold is to provide structural support, the matrix can also induce regenerative processes and facilitate incorporation through the action of biochemical signals, which are retained post processing.[13,14] As this novel class of materials is natural and resorbable, regeneration occurs with less inflammation and scar formation than with traditional synthetic options.

[†]Both authors equally contributed to this work as joint first authors.
[‡]Both authors equally contributed to this work as joint last authors.
Correspondence to: C. Neville; e-mail: neville@helix.mgh.harvard.edu

The mechanisms and biomaterial properties responsible for optimal incorporation and tissue repair are still being investigated with the aim of fostering continued improvement in clinical outcome.

Optimization is challenging as many processing steps are required for product manufacturing. Critical steps may include chemical decellularization using detergents, alkali and acidic solutions, proteolytic enzymes, thermal treatment or mechanical agitation, with subsequent crosslinking, dehydration, and sterilization.[15–17] To generate unique materials for improved soft tissue regeneration, each manufacturer has developed proprietary protocols, which markedly impact the resulting composition and mechanical properties.

Biological properties of ECM-derived materials also strongly impact the type and degree of the immune response, the recruitment and infiltration of host cells, and the eventual incorporation and remodeling of the scaffold into regenerated tissue. Scaffold incorporation and remodeling are lengthy processes, requiring several weeks or months. Interest exists in developing a better understanding of scaffold parameters that impact cellular incorporation and quality of outcome.[18,19] We recently reported a comparison of several similar dermis-derived biological scaffolds in a panel of *in vitro* assays.[20] These materials have principally been used for hernia repair and pelvic floor reconstruction, which require significant strength to support tissue repair.[21]

The success in abdominal wall reconstruction has led to interest in using ECM-derived materials in other reconstructive procedures, including eyelid, nasal, burn, lower extremity wounds, and breast.[21–26] Significant strength is not the primary design criteria for these materials. Rather flexibility, good incorporation, and low propensity for inciting fibrosis are required for generation of aesthetic results. In the present study, an *in vitro* assay panel was used to investigate several commercially-available and clinically-used surgical scaffold products, designed for applications such as breast reconstruction that simultaneously require strength and flexibility to support tissue regeneration.[27] In this study, the impact of these materials on early cell recruitment and infiltration was explored as these properties are essential for successful scaffold integration and tissue regeneration.

MATERIALS AND METHODS

Overview of experimental design

Five commercially available FDA-cleared surgical scaffold products, derived from different tissue and species sources, were investigated for intrinsic properties that support basic cellular physiological responses underlying tissue repair and regeneration. The products were received in their original package and were handled according to manufacturers' instructions. In addition, Gelfoam was included as a control as an example of highly processed, denatured collagen derived from porcine dermis (Table I). The scaffold materials were evaluated for ability to support cell proliferation, apoptosis, migration, chemotaxis, and cell attachment *in vitro*, and cell infiltration in a chick chorioallantoic membrane (CAM) assay. Many materials displayed sidedness which was easily identified based on surface texture. In the invasion and CAM assays, which were impacted by sidedness, the scaffolds were oriented so that the rougher, more porous side was adjacent to the infiltrating cells.

TABLE I. Surgical Scaffold Biomaterials

Material	Species	Tissue	Company
AlloDerm	Human	Dermis	LifeCell
Gelfoam	Porcine	Dermis	Pfizer
Meso BioMatrix	Porcine	Mesothelium	DSM Biomedical
OASIS	Porcine	Submucosa	Cook Biotech
Surgisis	Porcine	Submucosa	Cook Biotech
Veritas[a]	Bovine	Pericardium	Synovis

[a] Veritas supplied hydrated. All others supplied dry/desiccated.

Scanning electron microscopy

For scanning electron microscopy (SEM), all dry samples were sputter coated with gold (SC7620 Sputter Coater, Quorum Technologies, UK). Hydrated Veritas material was fixed in 10% buffered formalin and dehydrated in ethanol and bis(trimethylsilyl)amine (HMDS) prior to SEM. Both the top and bottom surfaces and a sharply cut cross section of each material were imaged. Imaging was performed on S570 SEM (Hitachi High Technologies, Schaumburg, IL) at 15 kV accelerating voltage.

Conditioned media preparation

The cytokines or matricryptic peptides that comprise eluted components may impact scaffold cellularization and remodeling.[28] In addition, the biocompatibility of biomaterials could be affected by residual chemicals remaining after the decellularization process.[29] All materials were sterilely processed in parallel in a blinded fashion. Each biomaterial was weighed, minced with a sterile razor blade and fine scissors, and placed in separate wells of six-well plates. Serum-free Dulbecco's Minimum Essential Medium (DMEM) (Life Technologies, Grand Island, NY) was added to each material to obtain a concentration of 50 mg biomaterial/mL medium and incubated at 37°C and 5% CO_2 on a rotator at 30 rpm. Medium not exposed to biomaterial was simultaneously processed and served as a control. After 24 h incubation, the media were cleared of materials in low-binding microcentrifuge filtration tubes (Costar Spin-X 0.22 μm cellulose acetate, Millipore, Danvers, MA) at 16,000 *g* for 10 min. Additional control medium was added to achieve a final concentration of 25 mg material/mL medium. The dry weight of pre-hydrated Veritas was estimated to be 20% of wet weight.

Protein concentrations of conditioned media were determined using the Pierce Micro BCA Protein Assay (#23235, Thermo Scientific) and measured on a NanoDrop 2000 spectrophotometer. Bovine serum albumin was used to generate standard curves.

Cell lines

NIH/3T3 fibroblasts (ATCC, Manassas, VA) were used for proliferation studies. Apoptosis was studied with primary human umbilical vein endothelial cells (HUVECs, Cascade

Biologics, Portland, OR) as they possess a significant apoptotic response through the caspase 3 signaling pathway.[30] Highly migratory human breast adenocarcinoma cell line MDA-MB-231 (ATCC, Manassas, VA) was used for migration and chemotaxis studies.[31] Human foreskin fibroblasts (HFFs, obtained from Dr. M. Detmar, MGH) were used for the cell adhesion assay. All cells except HUVECs were cultured in DMEM supplemented with 10% fetal bovine serum (FBS, Sigma Aldrich, St. Louis, MO) and 1% penicillin/streptomycin (Life Technologies). HUVECs were grown in endothelial growth medium (EGM, Lonza, Switzerland). Unless otherwise indicated, all experiments were performed in standard incubator conditions at 37°C and 5% CO_2.

In vitro assays with conditioned medium

Previously described *in vitro* assays have been refined.[20] All the material-conditioned media were generated and evaluated in parallel in a blinded fashion. Serum-containing medium (complete medium, DMEM with 10% FBS) served as the positive control and serum-free medium as the negative control. Experiments were performed with three technical replicates and repeated independently three times. Images were obtained of three random 100x magnified-fields on Eclipse TE-2000 inverted microscope (Nikon, Japan).

Proliferation assay

NIH/3T3 fibroblasts were labelled with 1 μg/mL Hoechst 33342 (Life Technologies); and 1×10^3 cells were plated into each well of a 96-well plate. After three hours, cells attached, the medium was removed, the wells were rinsed twice with PBS, and 50 μL of each material-conditioned medium was added to wells (time = 0 h). Images were taken at 0 h and 24 h. The cells were counted and fold-change relative to time 0 h was calculated.

Apoptosis assay

Apoptosis was measured with the Apo-ONE Homogeneous Caspase 3/7 Assay (Promega, Madison, WI) following manufacturer's recommendations. HUVECs were plated in EGM at 2×10^3 cells per well in black-walled 96-well plates (#3603, Corning, Tewksbury, MA). After 3 h, the medium was removed, wells rinsed twice with PBS, and 50 μL of each material-conditioned medium was added. After 24 h, cells were rinsed with PBS and the enzymatic activity of the capase-3/7 marker was assessed in lysates using the chemiluminescent assay.

Cell migration assay

The scratch-wound assay was used to evaluate the ability of eluted factors to induce cell migration. MDA-MB-231 cells were plated at 50×10^3 cells per well of a 24-well plate. After 6 h, cells adhered and formed a confluent monolayer. A 1 mm wide 'scratch' was made with a 200 μL pipette tip. The debris and residual serum were removed by rinsing twice with PBS. Conditioned medium was then added (0.5 mL per well) and the scratch was imaged immediately and after 12 h of incubation. The migration distance was calculated as a difference between the initial and final scratch width divided by 2.

Chemotaxis assay

Following manufacturer's protocol, ChemoTx plates with 8 μm pore membranes (#101–8, Neuro Probe, Gaithersburg, MD) were used to assess the chemotaxis activity in the presence of conditioned medium. MDA-MB-231 cells were labelled with 5 μg/mL Hoechst 33342 for 10 min. The top of the membrane was seeded with 20×10^3 cells in 20 μL medium and 30 μL material-conditioned medium was added to the well. After 24 h incubation, migrated cells attached to the bottom of the membrane were imaged and counted.

Direct cell adhesion test

To preserve cell surface receptors, HFFs were harvested non-enzymatically with cell removal buffer (Hanks solution with 1 mM EDTA, 10% glycerol, 60 mM sodium acetate). Detached cells were labeled with 5 μg/mL Hoechst 33342 for 10 min and resuspended in growth medium at 1.5×10^5 cells/mL. Three disks of each scaffold material (3-mm diameter) were cut with a biopsy punch (Miltex, Plainsboro, NJ) and individually placed in 2 mL low-retention microcentrifuge tubes (#Max-820S, Phenix Research, Candler, NC) along with 1.5 mL cell suspension. The tubes were rotated at 60 rpm for 3 h in an incubator. The scaffolds were then submerged in PBS to remove unattached cells and fixed with 4% paraformaldehyde. The attached cells were imaged (3 images/side/sample) and counted, and the counts were normalized by image area.

Invasion assay

The chemoattractant invasion assay assessed cell migration within the scaffold materials. Three disks were punched (10-mm diameter) from each material and glued to 12-mm diameter Millicell (Millipore, Bedford, MA) cell culture inserts, replacing the original membranes. If the material displayed sidedness differences, the grossly rougher, more porous side was positioned "up". The highly migratory MDA-MB-231 cells (5×10^3 cells) were plated inside these modified cell culture inserts in serum-free medium. To induce migration through the scaffold materials, serum-containing medium was added outside the insert as a chemoattractant. To verify that a serum concentration gradient remained, protein concentrations in the media on both sides were measured using the Bradford protein assay after 24 h. The cell-seeded disks were detached from the insert, fixed, embedded in paraffin, and sectioned. Cells were stained with 4',6-diamidino-2-phenylindole (DAPI, Sigma Aldrich) and imaged. The images were divided into 10 equal horizontal zones, and the cells were counted in each zone. The percent of total infiltrating cells in each zone and the number of cells in each zone normalized by zone area were determined.

Chick chorioallantoic membrane assay

CAM assay was used as an *ex vivo* vital model to evaluate early stage cell infiltration and neo-vascularization.[32]

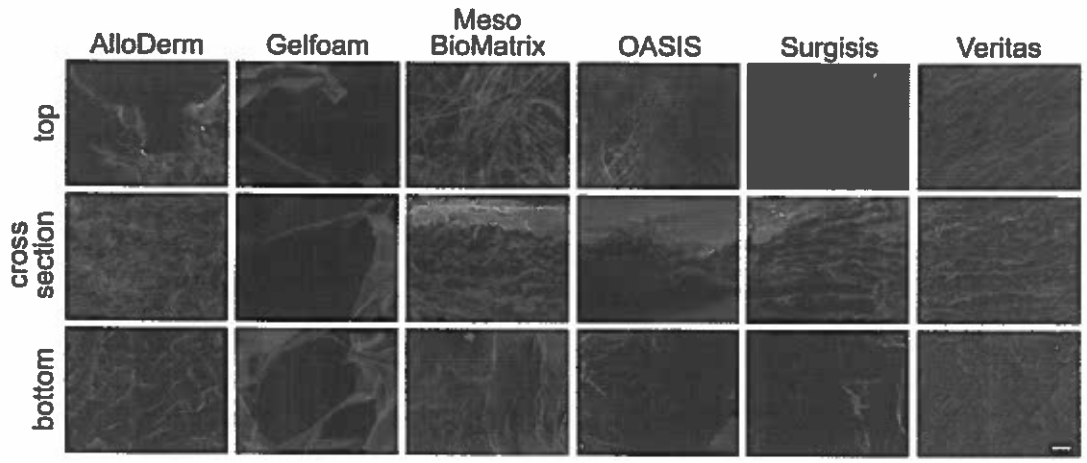

FIGURE 1. Surface and cross sectional characteristics of the biomaterials from SEM images. Scale bar = 50 μm.

Fertilized White Leghorn chicken eggs (Charles River Laboratories, North Franklin, CT) were incubated in a 38°C, 65% relative humidity egg incubator. Access to CAM was obtained as described before.[20] On day 3, a hole was created on the pointed end of each egg with an 18 g needle; 2–3 mL albumin was removed by syringe. On day 4, the viability of the embryo was inspected through a 1 cm^2 window in the shell, cut with a Dremel rotary tool. After inspection, the hole was sealed with cellophane tape. On day 7, disks of each scaffold material were punched (5-mm diameter) and briefly hydrated in PBS. Six eggs were used for each material. A single disk was placed on each CAM, with the rougher side "down" for materials with sidedness, and the egg shell was resealed. On day 14, the window was enlarged to permit photographing the material *in situ*. The material and surrounding membrane were removed, fixed in 10% formalin, paraffin embedded, sectioned, and stained with hematoxylin and eosin (H&E) or DAPI. Stained sections were imaged and cell infiltration was assessed for each material from cell counts normalized by image area.

Statistical analysis

One-way analysis of variance (ANOVA) was used to determine differences between groups for each assay. Tukey's *post hoc* test was used to determine differences between pairs, with $p < 0.05$ considered significant.

RESULTS

We investigated several commercially-available surgical scaffold materials derived from the ECM of a variety of tissues. Basic biological properties that contribute to the repair response and scaffold incorporation were assessed. Specific assays were used to evaluate cell proliferation, apoptosis, migration, and chemotaxis with each material-conditioned medium. A direct attachment assay was conducted to detect the cell adhesion potency of each material. The CAM assay was used to evaluate early stage cell infiltration and collagen remodeling *in vivo*.

Scaffold characterization

SEM was used to assess the physical character of the scaffolds (Figure 1). OASIS presented surfaces without clear differences. Both surfaces were smooth and without openings or pores exposing the interior. AlloDerm and Veritas also had top and bottom surfaces that were similar, but with a somewhat rougher texture than OASIS. Meso BioMatrix and Surgisis were similar, with one surface smooth, dense, and compacted while the obverse was fibrous and discontinuous. Cross sections revealed a trilayered structure for OASIS and a multilayered structure for Surgisis, both derived from porcine submucosa. The interior of the AlloDerm and Veritas materials were of a continuous dense fibrous nature. Meso BioMatrix was also homogenous and had significant porosity throughout its cross section. Gelfoam possessed highly porous surfaces and cross sections, with pore diameters significantly greater than the other scaffold materials.

Proliferation

A set of conditioned media was examined for extracted molecules that could support cellular processes. The mean protein concentrations (mg protein/mL conditioned medium) in scaffold-conditioned media were: AlloDerm 1.22 ± 0.22, Gelfoam 2.27 ± 0.20, Meso BioMatrix 1.18 ± 0.15, OASIS 1.53 ± 0.09, Surgisis 1.33 ± 0.09, and Veritas 1.56 ± 0.10. Meso BioMatrix and OASIS supported the proliferation of NIH/3T3 fibroblasts to a greater extent that the other biomaterials, with no significant difference between these materials [Figure 2(A)]. Cell number increased in Gelfoam-conditioned medium but significantly less than that in Meso Biomatrix and OASIS-conditioned media. Although cultures in Veritas-conditioned medium had a slight decrease in mean cell number, this decrease was not statistically significant. However, cell number decreased upon exposure to medium conditioned with AlloDerm and Surgisis.

Apoptosis

Our preliminary experiments confirmed that HUVECs are particularly sensitive to mitogen withdrawal, leading to

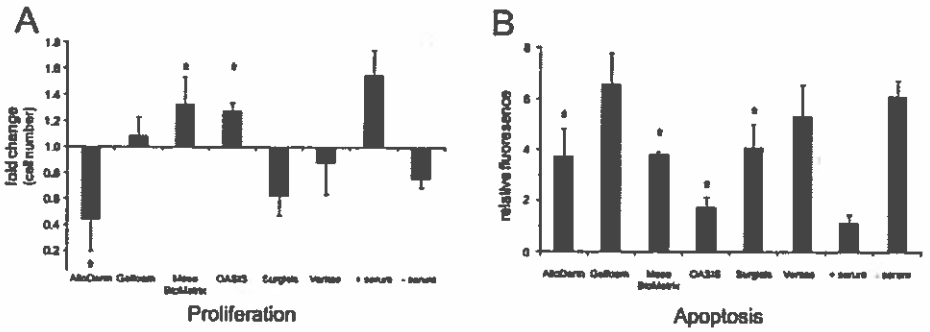

FIGURE 2. Cell cycle response to biomaterial-conditioned medium. A: Proliferation. NIH/3T3 fibroblasts, stained with Hoechst 33342, were imaged prior to and after culturing in conditioned-medium for 24 h and fold-change plotted. B: Apoptosis. After culturing HUVECs in serum-free medium for 24 h, recovery from stress-induced apoptosis was initiated by replacing with conditioned medium. After 24 h additional culture, enzymatic activity of caspase 3/7 was measured. For both (A) and (B), $n = 3$ technical replicates, repeated independently three times, and *, $p < 0.05$ relative to –serum conditions.

apoptosis (programmed cell death), a common cellular response to stress (data not shown). Serum-containing medium largely alleviated the response as caspase levels decreased to sixfold less than that in HUVECs maintained in serum-free conditions [Figure 2(B)]. OASIS-conditioned medium was almost as effective as serum at repressing the apoptotic response; AlloDerm, Meso BioMatrix, and Surgisis had intermediate activity. Apoptotic-inducing activity of Veritas and Gelfoam-conditioned media were not significantly different from serum-free medium.

Cell migration

Serum-free medium showed minimal ability to induce cellular migration into the cleared path, while inclusion of serum induced considerable mobility [Figure 3(A)]. Among the conditioned media, only that of OASIS and Meso BioMatrix showed a statistical improvement over serum-free medium.

Chemotaxis

Without chemotactic-inducing signals, MDA-MB-231 cells remained relatively immobile [Figure 3(B)]. Serum-containing medium with its chemoattractant signals induced cell migration. Among the materials, only Meso BioMatrix provided significant recruitment signals, performing similarly to serum. Both OASIS- and Veritas-conditioned media demonstrated some activity, while media conditioned with AlloDerm, Gelfoam, and Surgisis behaved like serum-free medium and displayed no chemoattractant properties.

Direct cell adhesion test

Only OASIS and Gelfoam did not display sidedness in this assay; all others had a statistical difference between the numbers of cells attached to opposite sides (Figure 4). Meso BioMatrix outperformed other materials in facilitating cell attachment.

Invasion assay

Material thickness was determined and found to range from ~200 μm for OASIS to 2500 μm for Gelfoam [Figure 5(A)]. The ability of the scaffold materials to support invading cells varied considerably [Figure 5(B)]. High numbers of cells were evenly distributed across the scaffold thickness in the highly porous Gelfoam. Meso BioMatrix was the only surgical material with cells observed throughout the full thickness of the material. OASIS, and to a lesser degree, AlloDerm, had cells that partially penetrated into the material. Cells attached without penetration to both Surgisis and Veritas.

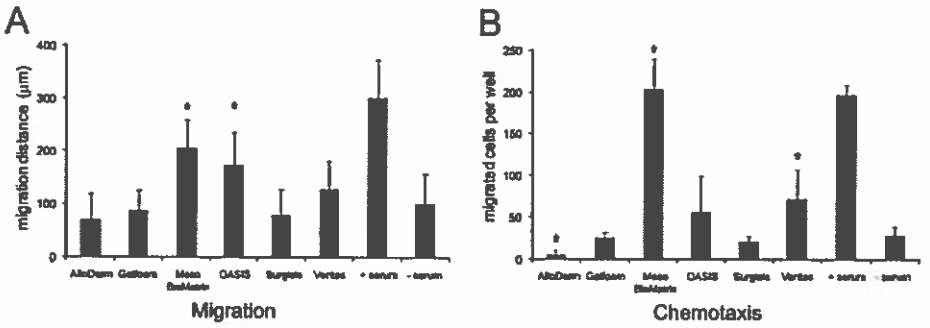

FIGURE 3. Cell migration response to biomaterial-conditioned medium. A: Migration. Induction of migration of MDA-MB-231 cells by conditioned media was evaluated in a scratch-wound assay. The migration distance was calculated to be one-half of the average difference between the initial and remaining widths of the cell-free path. B: Chemotaxis. The number of MDA-MB-231 cells was determined which migrated through the membrane in response to a conditioned media gradient. For both (A) and (B), $n = 3$ technical replicates, repeated independently three times, and *, $p < 0.05$ relative to –serum conditions.

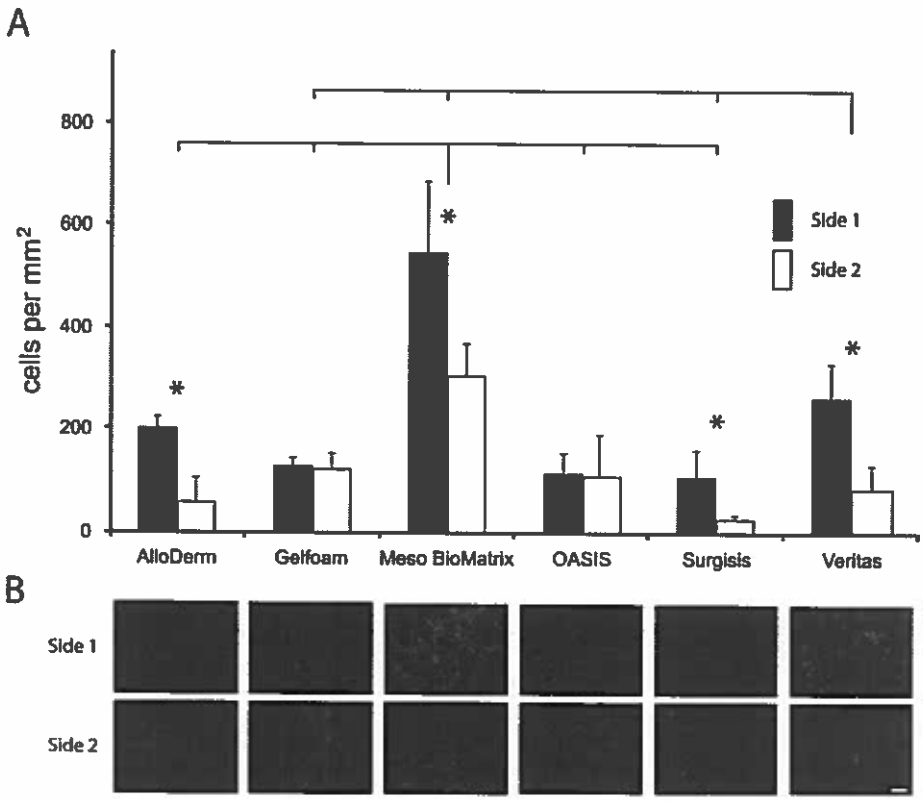

FIGURE 4. A: Cellular adhesion to biomaterials by Hoechst 33342-labelled HFFs was assessed. B: ECM sidedness was characterized by significantly different cell numbers attached to two sides of a biomaterial. For each material, $n = 3$. Scale bar = 50 μm. Side 1 and side 2 were compared for each material; *, $p < 0.05$. All bracketed data, $p < 0.05$. [Color figure can be viewed in the online issue, which is available at wileyonlinelibrary.com.]

Chick chorioallantoic membrane assay

Material disks were placed on the developing CAM [Figure 6(A,B)]. Cell infiltration [Figure 6(C)] was determined from H&E and DAPI stained sections [Figure 6(D,E)]. The highly porous Gelfoam demonstrated the greatest cell infiltration, with relatively homogenous cell distribution throughout all samples. OASIS and Meso BioMatrix had similar numbers of penetrating cells (no statistical difference relative to Gelfoam), although the cell distribution was densest near the proximal surface. Moderate ingrowth was supported by Veritas, while it was negligible for Surgisis and AlloDerm.

DISCUSSION

Surgical mesh scaffolds are increasingly being utilized to promote soft tissue repair and regeneration in a variety of clinical applications. Originally developed using synthetic polymers, surgical meshes provide strong support but incite a significant inflammatory response and some are non-resorbable. Resorbable synthetic materials can yield poor clinical outcomes as degradation products can induce chronic inflammation and fibrosis. Biological scaffolds derived from mammalian tissues have been developed as a replacement for these synthetic meshes. These scaffolds can impart the required support to the healing tissue and integrate with the native tissue while remodeling. Decellularized ECM surgical mesh products have the potential to facilitate cell attachment and invasion and can play an instructive role in tissue regeneration.[3,33,34] The choice of tissue origins and processing procedures provide opportunities to tailor material properties. The properties which influence biocompatibility and tissue interactions have not been previously assessed.

In this study, we characterized the biological activity of five clinical ECM-derived products developed for soft tissue repair in applications where aesthetic outcome is critical. These materials were produced using proprietary processes and distinct tissue sources so the resulting commercial ECM-derived surgical scaffold materials have unique properties and characteristics. Using an *in vitro* panel of assays, the abilities of these materials were assessed to retain biological activity and to mediate cell infiltration, an important component of the regenerative process.

The assays were collectively designed to assess the impact of retained soluble substances, which could potentially signal surrounding cells and tissues, and material architecture, which impacts invasion of the mobilized cells. The fibrous components of ECM sequester signalling molecules such as growth factors and cytokines. These factors are released during regeneration to induce cell proliferation,

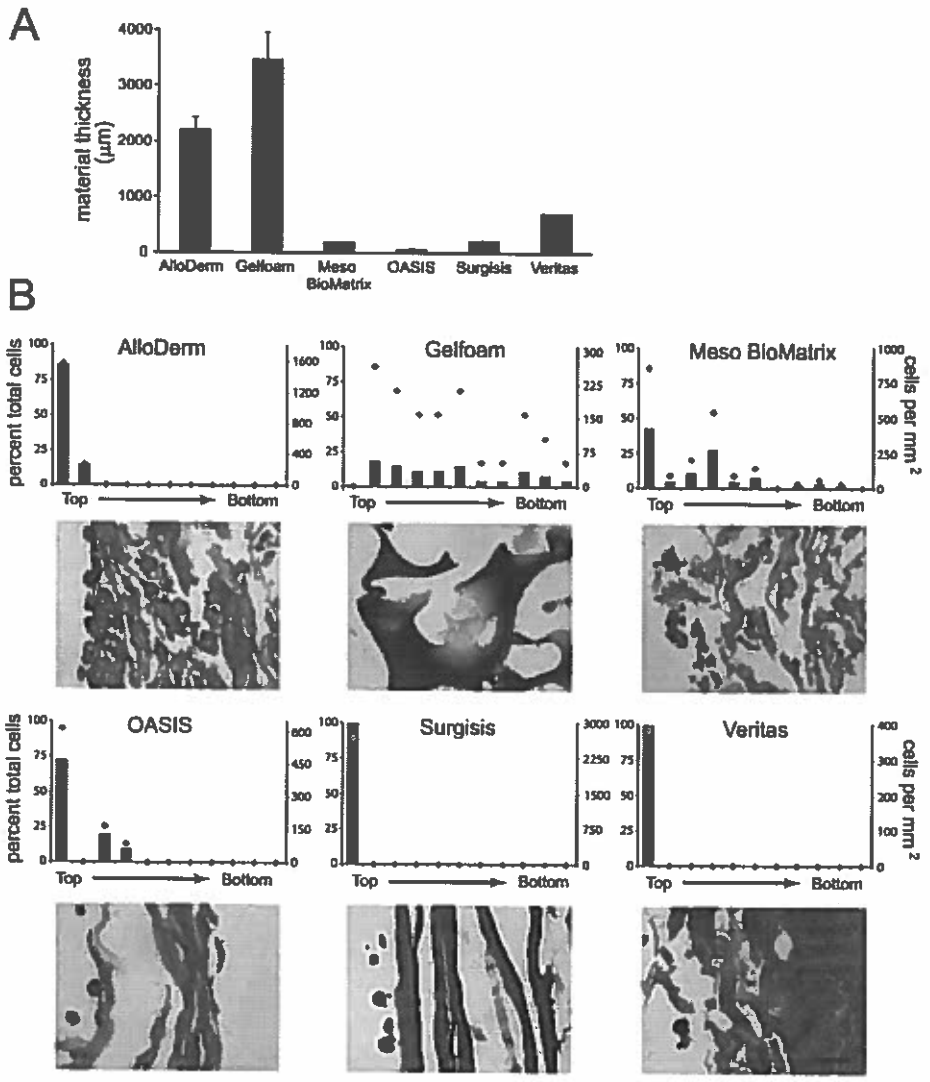

FIGURE 5. Cellular invasion. A: Average thickness of each biomaterial. B: Cell invasion into biomaterials was evaluated where cross sections were divided into 10 equal zones. The percent total cells (black bars to left y-axis) and cell density (diamonds to right y-axis) were plotted as function of the zone. For each material, $n = 3$. Scale bar = 50 μm. [Color figure can be viewed in the online issue, which is available at wileyonlinelibrary.com.]

migration and recruitment from nearby tissues. Because these factors are small and labile, they are easily lost or inactivated during material processing.[13] In addition, residual processing chemicals can impact surgical scaffold material biocompatibility.

The presence and biological activity of these soluble components in the scaffold materials were assessed through conditioned medium studies. Cell activities that are the basis of development and regeneration were evaluated, using cell types that are sensitive indicators for the assayed properties. The tissue-derived materials displayed a range of responsiveness in our assays. No correlation was observed between total amount of extracted protein and response to conditioned media for any of the assays; measured differences were likely due to elution of specific proteins and/or non-protein components.

An additional clinical material, Gelfoam, although not a surgical scaffold, was included as a control. It is a highly purified and denatured collagen product derived from porcine dermis and does not retain significant biological activity. Gelfoam-conditioned medium demonstrated little or no support for proliferation, mobilization and chemotaxis, nor did it mitigate apoptosis. However, its highly open, interconnected pore structure was highly supportive of integration.

Medium conditioned with Meso BioMatrix best supported cell migration and chemotaxis signaling. No other material demonstrated both activities, although OASIS and Veritas showed moderate ability to induce chemotaxis. Apoptosis attenuation was best supported by OASIS, followed by AlloDerm, Meso BioMatrix, and Surgisis. Meso BioMatrix and OASIS were the only materials which supported cell proliferation.

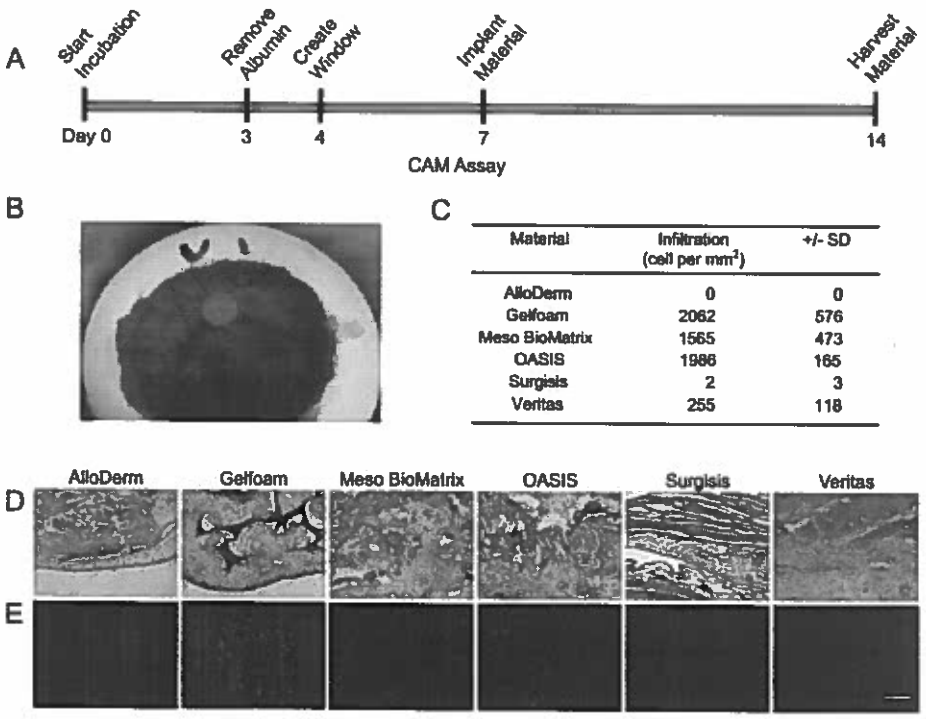

Material	Infiltration (cell per mm²)	+/- SD
AlloDerm	0	0
Gelfoam	2062	576
Meso BioMatrix	1565	473
OASIS	1986	165
Surgisis	2	3
Veritas	255	118

FIGURE 6. A: Timeline of CAM assay and (B) a biomaterial disk on CAM. C: Cells invading at least 100 μm into biomaterial were counted. D: H&E-stained biomaterial sections demonstrate material integration with the surrounding CAM and the invading cells. E: DAPI staining identifies invading cells. For each material, $n = 6$. Scale bar = 50 μm. [Color figure can be viewed in the online issue, which is available at wileyonlinelibrary.com.]

All materials except OASIS displayed sidedness with respect to cell attachment, with differences ranging from 1.8-fold for Meso BioMatrix to 4.1-fold for Surgisis. A "side" of each material was easily identified based on gross surface roughness and was verified in paraffin embedded sections as the side with greater open porosity (data not shown). Sidedness differences, which could impact optimal orientation in clinical applications, likely derive from the natural asymmetry of surface porosity in the starting material rather than an effect of material processing. One of the surfaces of Meso BioMatrix demonstrated superior cell attachment. Even the less cell-friendly side of Meso BioMatrix outperformed all others but Veritas' optimal side. Differences in inherent structural properties also impacted cell infiltration in the invasion and CAM assays; for these assays, each material was oriented so that cells would enter the rougher, more porous side of the scaffold. OASIS, followed by Meso BioMatrix, supported cell infiltration almost equal to that of the highly porous Gelfoam. In addition, Veritas showed some integration with the CAM tissue. While cell infiltration was observed throughout the OASIS and Meso BioMatrix materials, cells remained at the periphery for Veritas. However, the dense AlloDerm and Surgisis architectures likely prevented cell penetration in the CAM assay.

Certain caveats exist in interpreting this study. The regenerative process is complex and incompletely understood. Our *in vitro* assays do not fully mimic conditions during clinical application, but they do reflect many processes important for tissue regeneration. As a panel, they quantitatively characterize biological properties that would be difficult to assess *in vivo*. Biologic responses are the integration of many signals; both the absolute concentration and relative ratio of multiple factors or signal inputs can be important for inducing a particular response. The cell-based assays presented here do not identify specific cytokines or factors eluted into conditioned medium. However, they do present an advantage over ELISAs or similar biochemical assays as they characterize the effects of factors that have maintained bioactivity after decellularization. Further validation of the findings presented here is planned with follow-up *in vivo* studies.

In conclusion, our study showed that biologic surgical scaffolds derived from decellularized ECM have unique properties. Basic scaffold architecture led to pronounced differences in cell infiltration; without infiltration, the scaffold acts as a barrier rather than supporting integration at the wound site. Also, significant differences existed in the activities of eluted components to promote cell migration, proliferation, and chemotaxis. These results indicate that both biologic and structural properties should be carefully assessed during the development of new products and applications for this important class of biomaterials.

ACKNOWLEDGMENTS

The authors thank Brad Liskey and Ryan Phillips for their help with SEM, and Chris Bowley for reviewing the protocols. Xiao Luo, M.D. was the recipient of a national scholarship from the China Scholarship Council.

REFERENCES

1. Ansaloni L, Catena F, Coccolini F, Negro P, Campanelli G, Miserez M. New "biological" meshes: The need for a register. The EHS Registry for Biological Prostheses. Hernia 2009;13:103–108.
2. Badylak SF. The extracellular matrix as a scaffold for tissue reconstruction. Semin Cell Dev Biol. 2002;13:377–383.
3. Hodde J. Extracellular matrix as a bioactive material for soft tissue reconstruction. ANZ J Surg. 2006;76:1096–1100.
4. Smart NJ, Marshall M, Daniels IR. Biological meshes: A review of their use in abdominal wall hernia repairs. Surgeon 2012;10: 159–171.
5. Badylak SF. The extracellular matrix as a biologic scaffold material. Biomaterials 2007;28:3587–3593.
6. Badylak SF. Xenogeneic extracellular matrix as a scaffold for tissue reconstruction. Transpl Immunol 2004;12:367–377.
7. Hoganson DM, O'Doherty EM, Owens GE, Harilal DO, Goldman SM, Bowley CM, Neville CM, Kronengold RT, Vacanti JP The retention of extracellular matrix proteins and angiogenic and mitogenic cytokines in a decellularized porcine dermis. Biomaterials 2010;31:6730–6737
8. Hoganson DM, Owens GE, O'Doherty EM, Bowley CM, Goldman SM, Harilal DO, Neville CM, Kronengold RT, Vacanti JP. Preserved extracellular matrix components and retained biological activity in decellularized porcine mesothelium. Biomaterials 2010;31: 6934–6940.
9. Ota T, Gilbert TW, Schwartzman D, McTiernan CF, Kitajima T, Ito Y, Sawa Y, Badylak SF, Zenati MA. A fusion protein of hepatocyte growth factor enhances reconstruction of myocardium in a cardiac patch derived from porcine urinary bladder matrix. J Thorac Cardiovasc Surg 2008;136:1309–1317.
10. Shevach M, Soffer-Tsur N, Fleischer S, Shapira A, Dvir T. Fabrication of omentum-based matrix for engineering vascularized cardiac tissues. Biofabrication 2014;6:024101
11. Teicher EJ, Madbak FG, Dangleben DA, Pasquale MD. Human acellular dermal matrix as a prosthesis for repair of a traumatic diaphragm rupture. Am Surg 2010;76:231–232.
12. Wolf MT, Daly KA, Reing JE, Badylak SF. Biologic scaffold composed of skeletal muscle extracellular matrix. Biomaterials 2012; 33:2916–2925
13. Chun SY1, Lim GJ, Kwon TG, Kwak EK, Kim BW, Atala A, Yoo JJ. Identification and characterization of bioactive factors in bladder submucosa matrix. Biomaterials 2007;28:4251–4256.
14. Voytik-Harbin SL, Brightman AO, Kraine MR, Waisner B, Badylak SF. Identification of extractable growth factors from small intestinal submucosa. J Cell Biochem 1997;67:478–491.
15. Arenas-Herrera JE, Ko IK, Atala A, Yoo JJ. Decellularization for whole organ bioengineering. Biomed Mater 2013, 8:014106.
16. Gilbert TW. Strategies for tissue and organ decellularization. J Cell Biochem 2012;113:2217–2222.
17. Mancuso L, Gualerzi A, Boschetti F, Loy F, Cao G. Decellularized ovine arteries as small-diameter vascular grafts. Biomed Mater 2014;9:045011.
18. Burugapalli K, Thapasimuttu A, Chan JC, Yao L, Brody S, Kelly JL, Pandit A. Scaffold with a natural mesh-like architecture: Isolation, structural, and in vitro characterization. Biomacromolecules 2007;8:928–936
19. Lee SJ, Atala A. Scaffold technologies for controlling cell behavior in tissue engineering. Biomed Mater 2013;8:010201
20. Kulig KM, Luo X, Finkelstein EB, Liu XH, Goldman SM, Sundback CA, Vacanti JP, Neville CM. Biologic properties of surgical scaffold materials derived from dermal ECM. Biomaterials 2013;34: 5776–5784.
21. Ibrahim AM, Ayeni OA, Hughes KB, Lee BT, Slavin SA, Lin SJ. Acellular dermal matrices in breast surgery: A comprehensive review. Ann Plast Surg 2013;70:732–738.
22. Sherris DA1, Oriel BS. Human acellular dermal matrix grafts for rhinoplasty. Aesthet Surg J 2011;31:95S–100S.
23. Hayek B1, Hatef E, Nguyen M, Ho V, Hsu A, Esmaeli B. Acellular dermal graft (AlloDerm) for upper eyelid reconstruction after cancer removal. Ophthal Plast Reconstr Surg 2009;25:426–429.
24. Salzberg CA, Dunavant C, Nocera N. Immediate breast reconstruction using porcine acellular dermal matrix (Strattice™): Long-term outcomes and complications. J Plast Reconstr Aesthet Surg 2013;6:323–328.
25. Dieterich M, Faridi A. Biological matrices and synthetic meshes used in implant-based breast reconstruction—A review of products available in Germany. Geburtshilfe Frauenheilkd 2013;73: 1100–1106.
26. Ibrahim AM, Koolen PG, Ganor O, Markarian MK, Tobias AM, Lee BT, Lin SJ, Mureau MA. Does acellular dermal matrix really improve aesthetic outcome in tissue expander/implant-based breast reconstruction? Aesthetic Plast Surg 2015;39:359–368.
27. National Library of Medicine, ClinicalTrials.org, 2015.
28. Ricard-Blum S, Ballut L. Matricryptins derived from collagens and proteoglycans. Front Biosci (Landmark Ed) 2011;16:674–697.
29. Reing JE, Brown BN, Daly KA, Freund JM, Gilbert TW, Hsiong SX, Huber A, Kullas KE, Tottey S, Wolf MT, Badylak SF. The effects of processing methods upon mechanical and biologic properties of porcine dermal extracellular matrix scaffolds. Biomaterials 2010;31:8626–8633.
30. Shioiri T, Muroi M, Hatao F, Nishida M, Ogawa T, Mimura Y, Seto Y, Kaminishi M, Tanamoto K. Caspase-3 is activated and rapidly released from human umbilical vein endothelial cells in response to lipopolysaccharide. Biochim Biophys Acta 2009;1792: 1011–1018.
31. Mathew AC, Rajah TT, Hurt GM, Abbas Abidi SM, Dmytryk JJ, Pento JT. Influence of antiestrogens on the migration of breast cancer cells using an in vitro wound model. Clin Exp Metastasis1997;15:393–399.
32. Ribatti D, Nico B, Vacca A, Presta M. The gelatin sponge-chorioallantoic membrane assay. Nat Protoc 2006;1:85–91.
33. Asarias JR, Nguyen PT, Mings JR, Gehrich AP, Pierce LM. Influence of mesh materials on the expression of mediators involved in wound healing. J Invest Surg 2011;242:87–98.
34. Junge K, Binnebösel M, von Trotha KT, Rosch R, Klinge U, Neumann UP, Lynen Jansen P. Mesh biocompatibility: Effects of cellular inflammation and tissue remodelling. Langenbecks Arch Surg 2012;397:255–270.